**Research Article**
Volume 14:01, 2025

**Molecular Biology: Open Access**

**ISSN: 2168-9547** **Open Access**

# Carbon/Copper Oxide Composite (CCOC) from Date Palm Leaves, (*Phoenix Dactyliferous* L.), Tropical Fruit, Mata Kucing Seeds (*Euphoria Malaiensis*) and Cu Powder

**Fatima Musbah Abbas[1,3]*, Ahlam Khalofa[2], Hanan Musbah Abbas[3] and Abubaker Elsheikh Abdelrahman[4]**

[1]*King Khalid University, Collage Science and Art, Dhahran Aljanoub, Abha, Saudi Arabia*
[2]*Department of Biology, King Khalid University, Abha, Saudi Arabia*
[3]*National for Research Remote Sensing Authority, Khartoum, Sudan*
[4]*Associate Professor, Director of Act Centre for Research, Singa, Sudan*

## Abstract

Carbon/Copper Oxide Composite (CCOC) was prepared by carbonization mixtures of Pre-Carbonized Date Palm Leaves (PCDPLs), tropical fruits Mata Kucing Seeds (Euphoria Malaiensis) (MKS) and Copper (Cu) powder in a nitrogen environment. The obtained CCPs were characterized by XRD and ultrasonic techniques in terms of crystallite dimensions (d002, Lc and La), Lattice Constant (a), Surface Area (SSA), Spring Length (SL), Young's Modulus (YM) and Electrical Conductivity (EC). Results of XRD profiles showed that the structure of the composite produced is polycrystalline with a two-phase structure that is formed of the composite carbon and copper oxide. Possibly the copper oxide is synthesized due to decomposition of Cu into nanoparticles' vapour during the carbonization process. The Crystallite dimension (d002, Lc and La), SAA and SL were found to change systematically with increasing PCDPLs% concentrations. The measurements of the lattice constant were found in an arrangement of 4.21Å-4.48 Å, which is close to that of the reviewed value (4.68 Å), proving the crystalline structure of copper oxides. The C. Yield and YM were increased with increase (MKs+Cu). The frequency dependent conductivity was successively analyzed by the Cole-Cole plot, indicating that lower conductivity behavior with little improvement with increasing (MKS+Cu) content.

**Keywords:** Carbon/Copper Oxide Composite • X-Ray diffraction • Crystallites dimensions • Crystallites parameters • Surface area • Spring length • Young's modulus • Cole-cole plot • Electrical conductivity • Mata kucing

## Introduction

Carbon composite materials are attractive for many applications, such as aerospace, engineering design [1], thermal applications, super capacitors [2], electrochemical capacitors, and energy storage devices [3], because of their low density, high heat conductivity, and superior mechanical and electrical qualities. The key benefit pertains to the chances of drastically decreasing weight and costs while keeping robust mechanical properties [1]. Generally, all carbon composites such as carbon brushes and carbon electrodes are produced by carbonization of carbonaceous precursor made from a mixture of materials such as petroleum coke, lampblack or natural graphite and metal powders with a binder such as pitch or resin.

The useful properties of the carbon fiber and carbon can be fabricated to join the metal and metal oxide compounds within their molecular matrix structure, such as aluminum-reinforced carbon fire [4], $MnO_2$- carbon nanocomposites and $MnO_2$-carbon nanoparticles [5]. Additionally, carbon/glass hybrid composites [6] and polymer reinforced carbon fiber [7]. Therefore, the most composite carbon electrodes were prepared by direct mixing of mechanical performance and electrical conductivity for the composite material for the thermoelectric application [8].

Solid carbon materials have frequently been produced in a variety of physical forms, from dependable items like powder, granules, and pellets, to expand their scope of industrial uses. Pellets are very useful since they are dense or have particle sizes that are solidly bonded together. Furthermore, the pellet form can give a more fundamental knowledge of the physical characteristics of carbon and the interactions that take place on its surface [9,10]. Other properties such as compressive yield strength, stiffness in compression, resistance to fatigue, corrosion, fracture toughness with possible manufacturing are key considerations [4,11].

Mechanical performance and electrical conductivity for the composite material, such as carbon and carbon Composites for thermoelectric Application, Aluminum Metal Reinforced Carbon Fiber [4], carbon/glass hybrid composites [6] and polymer reinforced carbon fiber [7]. In addition, composite carbon electrodes were prepared by direct mixing of manganese oxide ($MnO_2$) with carbon materials using binder to produce $MnO_2$-carbon nanocomposites and $MnO_2$-carbon nanoparticles [5].

The first part of the composite, which was prepared from biomass, agricultural and industrial waste, has also regained its economic benefits, as most of the waste is usually ignored and disposed of. Biomass materials have been utilized to develop carbon material such as Spinach leaves [12], pre-carbonized biomass residues [13], oil palm empty fruit bunches [5, 6], and soybean dregs [14] that can be used in many applications such as electric double layer capacitors, and electromagnetic wave absorption. As a result, several attempts have been made to enhance the characteristics of carbon, such as pre- carbonizing at a low temperature and fine-grain powder grinding, which is crucial to enhancing the material's mechanical performance and self-adhesive qualities [10,15] thermal properties and carbonization temperature [15,16].

Among them, date palm leaves (*Phoenix dactyliferous* L.) biomass is categorized as lignocellulose material, which is composed of cellulose, hemicellulose, and lignin. The main products of this material are abundant, inexpensive, and have a high carbon content and low ash content. As an attractive precursor for the carbon material [10,15], phenol acid [17]. In addition, the date palm wood biomass shares some advantages as a composite

***Address for Correspondence:** Fatima Musbah Abbas, King Khalid University, College Science and Art, Dhahran Aljanoub, Abha, Saudi Arabia; E-mail: fmelamin@kku.edu.sa*



**Received:** 03 February, 2025, Manuscript No. MBL-25-162516; **Editor Assigned:** 05 February, 2025, PreQC No. P-162516; **Reviewed:** 18 February, 2025, QC No. Q-162516; **Revised:** 24 February, 2025, Manuscript No. R-162516; **Published:** 04 March 2025, DOI: 10.37421/2168-9547.2025.14.470

reinforcement to improve its mechanical or without chemical agents [18,19]. More recently, it has been used to prepare activated carbon and carbon pellets with a high surface area with excitable mechanical and electrical properties [10,15,20].

The second biomass that has been added is the tropical fruit seeds known as mata kucin (translated as 'cat's eyes' in English) from the species (*Euphoria Malaiense)* (MKs), which is of considerable economic importance as a source of food widely distributed in the tropical regions. Also, it has been used in medical applications such as treatment of excessive bleeding and sweating [18]. The fruit shells of the MKs and other tropical fruit bio-waste durian have been utilized to make activated carbon as an electrode active ingredient in the fabrication of the electrode of a double layer capacitor [21]. Therefore, MKs have been found suitable to be converted to a powder that can be pelletized without adding any binding agent.

The third part of the composite is metal oxides. The Copper Oxide ($Cu_2O$) compound refers to a p-type semiconducting material that has several potential practical applications, including spin dynamics, electron correlation effects, and high temperature superconductivity [22,23], biomedical [24] and surface coatings [25]. The CuO nanowire [26], carbon nanoflakes/CuO nanowires [27] and $\alpha$-$Fe_2O_3$ nanorods/ carbon nanotubes-graphene [28] were utilized as superior anodes for lithium-ion batteries. In addition, other metal oxides such as NiO nanosheet/carbon were fabricated to enhance the properties of the lithium storage property [29].

In the present work, the Carbon/Copper Oxide ($Cu_2O$) composite was prepared with a direct mixture of Pre-Carbonized Date Palm Leaves (PCDPLs), tropical fruit mata kucing (*Euphoria Malaiensis*) (MKS) and Copper (Cu) powder. It is commonly recognized that the intensity of X-ray interference provides relatively direct information on the arrangement of atoms in crystal structure and characterizes the dimensions of the crystallite ($d00_2$, Lc and La) of the graphitic like crystallites in carbon materials [10]. There are various mathematical models that have been used to correlate crystallite dimensions with elastic modulus *via* the estimated diagram of a cubic granular volume structure Figure 1 proposed by Emmerich FG [30], by supposing that the majority of the carbon granular structure is composed of microcrystalline graphite [10,11,31] and Specific Surface Area (SSA) as a class of X-ray diffraction applications [10].

Schematic diagram of cubic volume granular structure in two dimensional proposed by Boyer RR, et al. [11] (Figure 1). Therefore, analysis of the X-ray diffraction profiles of the composite pellets identified a Copper Oxide ($Cu_2O$) compound synthesized on the composite surface. Possibly due to decomposition of Cu particles to nanoparticles vapor reacted with oxygen or carbon dioxide as reviewed by many workers [1-4] as suggested in Figure 2. The oxygen or carbon dioxide and other violated components are expected to be released from the biomass during the pyrolysis mechanisms [3,5].

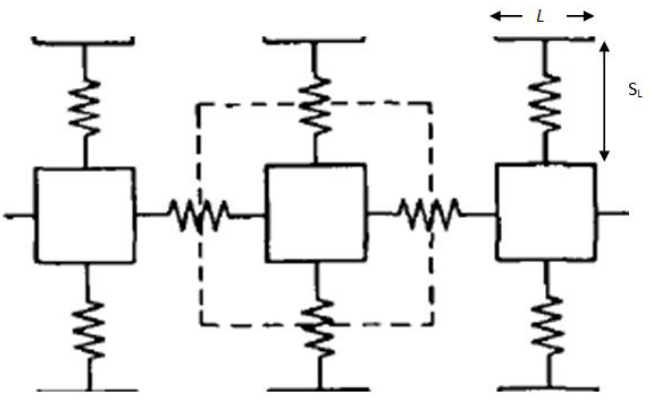


**Figure 1.** Schematic diagram of cubic volume granular structure in two dimensional proposed by Boyer RR, et al. [11].

Suggesting possible condensation of $Cu_2$ molecules and decompose to nanoparticles vapors in order to synthesis $Cu_2O$ in the composite surface (Figure 2). The aim of the present work mainly describes the preparation, structure, and characterize the crystallite dimensions (Interlays Spacing ($d00_2$) and Stacking Orders ($L_c$ and $L_a$), Lattice Constant (a), Specific Surface Area (SSA), Young's Modulus (YM), and Electrical Conductivity (EC) by applying LCR and Cole-Cole plot graphical Figure and theoretical Debye behavior [6-8] to understanding of the motilities carrier. The produced composite materials can be used as an electrode or current collector, depending on their specific qualities. To evaluate accuracy, the crystallite dimensions were calculated using an X- ray diffraction software, and the outcomes were compared to the review data that had previously been reported.

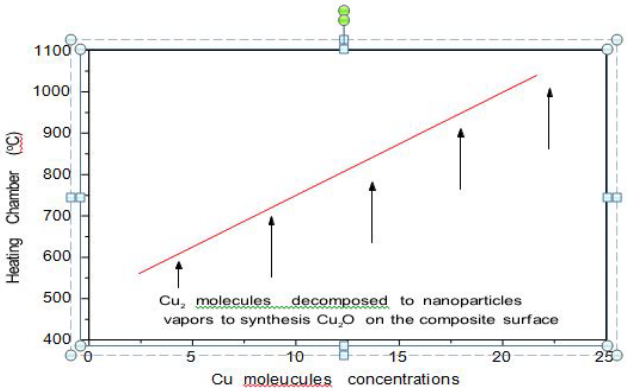


**Figure 2.** Suggesting possible condensation of Cu2 molecules and decompose to nanoparticles vapors in order to synthesis Cu2O in the composite surface.

## Materials and Methods

### Sample preparation

Leaves of Saudi Arabian date palm (*Phoenix dactylifera* L.) were collected from both rural and urban areas and parts of cities situated in southern regions. Then, the raw date palm leaves are chopped into small pieces and later thoroughly washed with hot water to remove dust particles (Figure 3). Then, the leaves were dried at 100 °C for 4 hours before vacuum carbonization was performed at 280 ℃ for 4 h which causes the leaves to shrink and disintegrate the microstructure of the lignocellulosic structure. The use of thermogravimetric analysis was done to determine the pyrolysis behavior of date wastes and date palm leaves [17,30]. Volatile and coke residues are the main volatiles gaseous products formed during the thermal degradation leading to loss of mass [17,32,33].

The Pre-Carbonized Date Palm Leaves (PCDPLs) (Figure 4) were of three different colors: medium brown, brown and dark brown, respectively. The PCDPL produced was then grounded by a ball milling process to a fine powder. The amount of PCDPL was 50 g for each milling setup for 50 hours of milling time to optimize self-adhesive properties. The grain powders are stored in clean self-sealing plastic bags in silica gel until used.

**Figure 3.** Date palm leaves cut into small size and pre-carbonized in a vacuum chamber at 280 ℃.

**Figure 4.** Date palm leaves.

## Mata Kucing (*Euphoria Malaiensis*) Seeds (MKS)

Tropical fruit Mata Kucing Seeds (MKS) were thoroughly washed and cut into small pieces, dried naturally in open air for one week, then soaked in one mole of sulphuric acid and then stirred for 3 hours and kept for 2 days. Following a two-day soak, the powder was dried for a further 24 hours at 100 , and the acid was removed with distilled water until the pH concentration reached 6. Similarly, the ball milled for 50 hours (h) to produce a fine grain powder to improve its self-adhesive properties. The obtained fine grain powder was mixed with copper powder by weight at a ratio of MKS: Cu=3:2.

## Composite preparation and carbonization processes

The PCDPls grain powder with particles of ≤ 10 micron and concentrations of 50%, 60%, 70%, 80%, 90%, and 100% (by weight) directly added to mixtures of MKS and Cu powder (supplier Aldrich company) in a weight ratio of MKS: Cu (3:2), having concentration of 10%, 20%, 30%, 40%, 50% (by weight) as shown in Table 1. These compounds were mixed manually and separated in a separate plastic container until use (Figure 5). One gram of these compounds was transformed into pellets by applying 12 metric tons of pressure without adding any binder. Prior to being carbonized at 1000 ℃ in a nitrogen atmosphere utilizing a multistep heating profile schedule intended as follows, every grain pellet demonstrated exceptional self-adhesive properties. The temperature was maintained at room temperature up to 375 ℃ for one hour, after which it ramped at a rate of 3 ℃ per minute up to 800 ℃ and subsequently at a rate of 5 ℃ per minute up to 1000 ℃, holding for five minutes [20].

Then the system was left to cool naturally to the room temperature. Next, the samples obtained were washed thoroughly with hot distilled water to remove impurities and then dried in an oven at 100 ℃ for four hours until a pH of 6 was achieved. The pellets' dimensions before and after carbonization was measured using a micrometer and the bulk density was measured as the weight of the sample divided by its volume. It is the average of five replicates of each sample and is represented as a function of PCDPLs % (Figure 6).

**Table 1.** Raw composite concentrations.

| PCDPLs % | Mata Kucing Seeds % | Copper (Cu) % by |
|---|---|---|
| 100 | 0 | 0 |
| 90 | 6 | 4 |
| 80 | 12 | 8 |
| 70 | 18 | 12 |
| 60 | 24 | 16 |
| 50 | 30 | 20 |

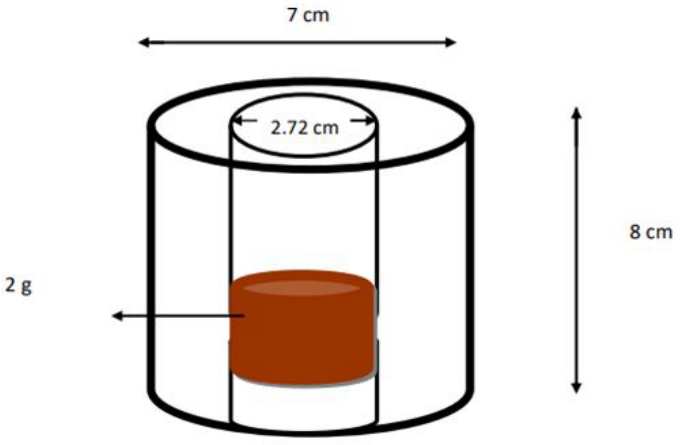


**Figure 5.** Pelletized molds used to prepare the pellets.

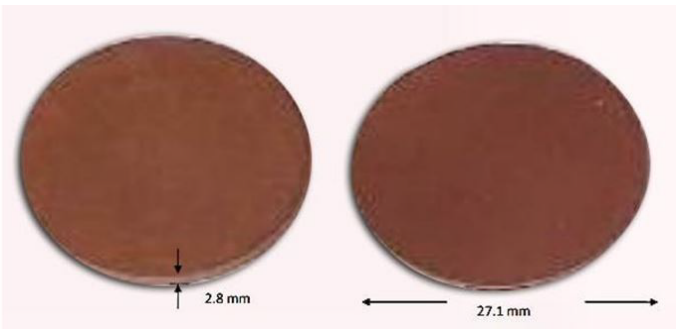


**Figure 6.** Pre-carbonized pellet.

## X-Ray Diffraction (XRD)

An X-ray diffraction experiment was conducted on CCOC pellets using a Rigaku D/Max- X-ray diffractometer with Cu-Kα radiation, at a scanning rate of 5s for every 0.1-step size at a diffraction angle of 2θ between 10° and 80° (Figures 3 and 4). The diffraction was analyzed using the Traces Varian 5 program from Diffraction Technology PTG LTD, Australia, to compute the crystallite dimensions such as stack height ($L_c$) and stack diameter ($L_a$) of graphite-like crystallites using Scherer's Equation (1) and Warren's correction for instrumental line broadening.

$$L = \frac{k}{\beta \cos\theta} \qquad (1)$$

Where θ is the scattering angle position, λ is the wavelength of X-ray diffraction, K is a shape factor which is equal to 0.9 for $L_c$ and 1.84 for $L_a$, β is the width of a reflection at half-height expressed in radians. The relationships between $d00_2$, and La can be deduced by assuming a well-known condition that for large $L_a$ and $1/L_a$ approaches zero, and that $d00_2$, $1/L_a$ should follow a linear Equation [9].

$$d_{002} = 3.35 + \frac{9.5}{La} \qquad (2)$$

## Scanning Electron Microscope (SEM)

The SEM micrograph was characterized for selected carbon composite sample using a S440-Leica Scanning Electron Microscope (SEM) instrument of magnification 5.00 $K_x$, with a Probe of 100 PA and EHT of 10.00 KV for selected composite sample braked into a small piece.

## Specific surface area

Then the specific surface area the CCOC can deduced from bulk density ($\rho$) and stacking height ($L_c$) [10] as

$$SAA = \frac{2}{\rho L_c} \qquad (3)$$

### Spring Length (SL)

The spring length (SL) between two cubic volume granular structures (Figure 1) is given as,

$$SL = L\left(\frac{1}{x^{\frac{1}{3}}} - 1\right) \qquad (4)$$

L is the cube root of the mean grain volume and is given as,

$$L = \left[\left(\frac{\pi}{4}\right)\left(L_a\right)^2 L_c\right]^{\frac{1}{3}}$$

X is the volume fraction given as

$$X = \frac{\rho}{P_{gr}} \qquad [11]$$

## Ultrasonic techniques

The ultrasonic velocity of the carbon pellets was measured before and after carbonization using the Ultrasonic Pulser-Receiver, Model 500 PR operated at 25 MHz at room temperature and the PICO instrument with the ADC-200 program. The pulsar section produced electrical pulses that were coupled through mating transducers to produce ultrasonic signals. Petroleum jelly was used as a coupling medium between the probe and sample. The ultrasonic signal and measure the Young's Modulus (YM) of a reference Glassy Carbon (GC) was used. The measured GC was close to the value given by the supplier with an error of <1%. The measured value of Young's Modulus (YM) for the one-dimensional form of the wave Equation is as following:

$$YM = \rho V^2 \qquad (5)$$

## Electrical Conductivity (EC)

The frequency dependent of the conductivity (real part, imaginary part) was carried out by e- Agilent E4980A precision LRC meter cell device (the Inductance [L], Capacitance [C], and Resistance [R] of an electrical component with option 001 (DC Measurements), by applying voltages from 0 to 5 V, with a Frequency (f) of range (0 MHz – 6.5 MHz) to characterize the conductivity behavior of the composite produced, and if it is applicable as electrode or current collector. The theoretical Debye behaviors and Cole-Cole plot in known [34-36].

# Results and Discussion

## X-ray diffraction

Figures 7 and 8, depict the X-ray diffraction pattern for the carbon composite pellets generated in the current study. The XRD patterns of the as prepared CCOC pellets are shown. Eight pronounced strong peaks at reflection plans (002), (110), (111), (100), (200), (111), (211) and (311) corresponding to diffraction angle (2 theta) of 25.9°, 28.7°, 36.4, 39.69°---40, 43.9, 50°.32, 53.25° and 63.20°, respectively, indicating polycrystalline structure (Figures 4 and 5). The peaks position labels and d- spacing are presented in Appendix (A). Generally, in the diffraction profile for all carbon composite pellets produced, there are three strong, sharp peaks at (002), (100), and (111), representing a characteristic of the graphite, while other diffraction peaks (110), (111), (200) (211) and (311) represent the dominant structure of $Cu_2O$ nanoparticle, a compound on the surface of the CCOCP pellets and the X-ray diffraction profiles of the $Cu_2O$ compound is given in Appendix (B).

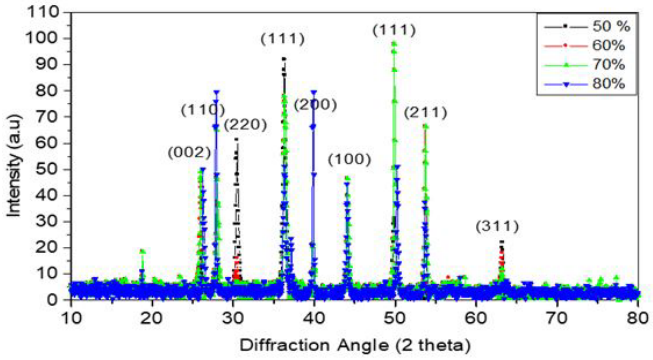


**Figure 7.** X-ray diffraction data for CCOC ((50%-80%) PCDPLs).

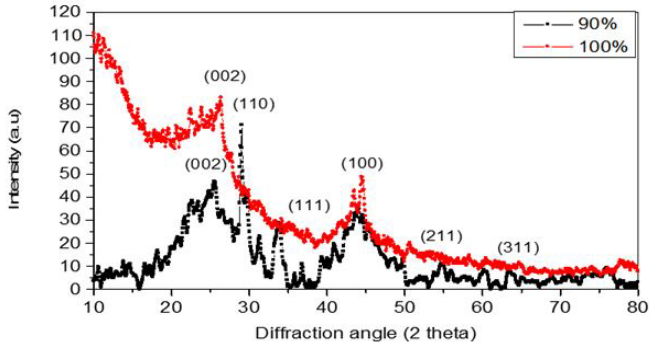


**Figure 8.** X-ray diffraction data for CCOC ((90%-100%) PCDPLs).

Figure 8, represents the X-ray diffraction profile of the CCOC pellets treated with (90%-100%) PCDPLs produced. The X-ray diffraction intensity of the untreated carbon sample (100 PCDPLs) at (002) and (100) reflection of Bragg's peaks, was broad with higher background intensities profiles, showing that the typical structure is turbostratic [10]. This diffraction intensity has been corrected to the background line intensity and fitted to the Gaussian distribution curve, to calculate crystallite by using trace diffraction programs. While CCOC treated with 90% was a broad intensity indication of lower crystalline dimensions with synthesis $Cu_2O$ compounds at (110), (111), (211) and (311) with lower diffraction intensity profiles. Table 2, show that the $d00_2$ for carbon structure composition in the CCOC is reduced with reduced PCDPLs% concentrations. It also shows that the stacking order lc and la increased by reducing PCDPLs% concentrations.

The X-ray results found that decreasing PCDPL% content tends to increase the crystal dimensions of the composite pellets. The X-ay diffraction results are obvious. The combination of Cu with biomass PCDPLs and MKs caused the factor to change the non-graphitic structure more graphitic and synthesize $Cu_2O$ due to decomposition of $Cu_2$ synthetic nanoparticle vapor during the pyrolysis process in the heating chamber as suggested in Figure 2. Work by Abdelrahman AE, et al. [37,38] reported that the energy release for $Cu_2$ molecule condensation is larger than the copper energy gap, then it is possible for particle growth of copper oxide by condensation of copper particle molecules ($Cu_2$) by the following reaction.

$Cu+CO_2$ $Cu_2$ O+ CO (1)

We consider the representation of the volatile components formed during component process such as carbon monoxide and oxygen could be responsible of the following reaction

$2Cu_2 + CO \quad 2Cu_2O + CO \quad (2)$

$2Cu_2 + O_2 \quad 2Cu_2O \quad (3)$

The XRD diffraction intensity showed the mean interlayer ($d00_2$) greatly decreased and the average crystallite dimensions ($L_a$ and $L_c$) were increased by increasing the MKS and Cu filler concentrations as shown in Table 3. They also showed that the interlayer spacing, $d00_2$, (3.42Å- 3.68Å) was greater than that for the pure graphite structure ($d00_2$=3.354 Å), indicating the microstructure of non-graphitic carbon structure. The relationship between $d00_2$ and 1/La is presented in Figure 9, and the data were fitted very well, with a slope of 9.33 Å2 close to that of the theoretical value (= 9.5 Å2) and a cut y-axis of 3.35 Å, which is in a good agreement with the Equation (2), and the fitting Equation is given

**Table 2.** PCDPLs%, d002 (Å), Lc (Å), La (Å) , SSA (m2/g and SL(Å) from the carbon structure composition in the CCOC.

| PCDPLs % | $d_{002}$ (Å) | $L_c$ (Å) | $L_a$ (Å) | SSA ($m^2/g$) | SL (Å) |
|---|---|---|---|---|---|
| 50 | 3.42 | 88.8 | 142.6 | 125.13 | 1248.50 |
| 60 | 3.43 | 79.6 | 125.1 | 155.58 | 0996.39 |
| 70 | 3.47 | 42.1 | 72.6 | 319.26 | 0197.46 |
| 80 | 3.49 | 34.3 | 57.1 | 444.77 | 0116.80 |
| 90 | 3.51 | 26.4 | 43.4 | 616.92 | 0056.31 |
| 100 | 3.68 | 12.6 | 32.2 | N | 0020.65 |
| Abbas FM, et al. [31] | 3.68-3.79 | 9.9 -10.9 | 30.8- 35.6 | | |
| Dolah BNM, et al. [40] | | | | 279 -656 | |
| Emmerich FG [30] | | | | | 003.72 |

**Note:** N is not measured

**Table 3.** Diffraction angle 2 theta, d- spacing, reflection plan (h k l) , chemical compound and lattice constant of the CCOC pellets.

| 2 Theta | d- spacing (Å) | h k l | Compound and Structure (CCOC) | Lattice Constant (Å) |
|---|---|---|---|---|
| 25.88 | 3.42 | 002 | CCP | |
| 26.04 | 3.42 | 002 | CCPs | |
| 26.24 | 3.39 | 002 | CCP | |
| 27.84 | 3.2 | 110 | Cu2O (Cubic) | 4.53 |
| 28.01° | 3.18 | 110 | $Cu_2O$ (Cubic) | 4.49 |
| 36.38° | 2.47 | 111 | $Cu_2O$ (Cubic) | 4.27 |
| 37.12 | 2.42 | 111 | $Cu_2O$ (Cubic) | 4.19 |
| 39.84 | 2.26 | 200 | $Cu_2O$ (Cubic) | 4.52 |
| 40.2° | 2.24 | 200 | $Cu_2O$ (Cubic) | 4.48 |
| 44.04 | 2.05 | 100 | CCPs | - |
| 44.36 o | 2.04 | 100 | CCPs | |
| 49.73° | 1.83 | 111 | CCPs | - |
| 50.24 | 1.81 | 111 | CCPs | |
| 53.3° | 1.72 | 211 | $Cu_2O$ (Cubic) | 4.21 |
| 63.3 | 1.47 | 311 | $Cu_2O$ (Cubic) | 4.87 |
| Average | | | | 4.45 |
| Review $Cu_2O$ (Robert) | | | | 4.68 |

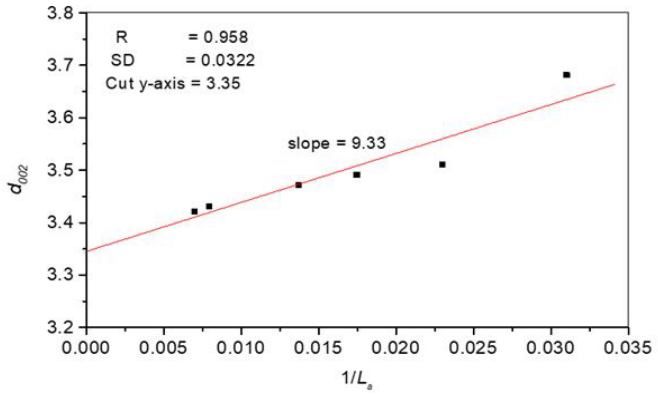


**Figure 9.** d002 *vs*. 1/La.

$$d_{002} = 3.35A^{\circ} + \left\{\frac{9.33}{L_a}\right\}A^{\circ} \quad (6)$$

However, our samples can be considered isotropic because, when the stack diameter ($L_a$) of the crystallite exceeds a certain diameter, the $d00_2$ becomes very dependent on 1/La. Indicating that the crystallite growth, improvement of the stacking diameter proceeds simultaneously with the change in $L_a$ by closed correlated factor of (9.5), as shown in Equation (2) and Equation (6).

## Specific Surface Area (SSA) and Spring Length (SL) between tow cubic granular structure

The Specific Surface Area (SSA) of CCOC pellets samples measured from Equation (4) are summarized in Table 2. The values were varied from 125.13 $m^2/g$ to 616.92 $m^2/g$. It is in the range of the activated carbon electrode from oil palm empty fruit bunches treated with Nitric Acid ($HNO_3$) [39] indicating that the SSA was increased with increasing PCDPLs % concentrations. It also shows that 90% and 80% PCDPLs give an acceptable SSA that can be used by many applications such as absorption catalyst and double layer capacitors.

Table 2 also summarizes the Spring Length (SL) between two cubic granular volumes calculated from Equation (4) displaying that the SL was enlarged up to

1248.5 (λ) for the composite prepared by 50% PCDPLs with reduction of the PCDPL's % content. Compared to our previous work on the activated carbon pellets from PCDPLs activated by potassium hydroxide, [10] the SI (i.e. 3.72 Å ≈ $d00_2$ (i.e. 3.71) was fluctuating and approximately equal to that of interlays spacing of activated carbon produced. The problem creates many collapses and cracks during the carbonization and the washing process. Therefore, we used the spring test following the microscopic cross-linking model proposed by Emmerich FG [30] to solve this problem. As a result, the composites produced are saved from crack, and we consider that owner composites can support thermal heating and tension. Next, we examine how this model is utilized to describe the mechanical properties of carbon material at the tiny level. If not, this is an alternative technique for microstructure characterization used in the production of carbon and composited carbon electrodes for thermo-thermal heating applications in order to prevent cracks or collapse.

SEM images of selected CCOC pellets were taken and are shown in Figure 10. The surface appearance of the carbon material can be affected by internal changes in the microstructure and all Figures confirm slight variations in shape. The surfaces of the samples were composed, with different porosity, particle sizes, and intergrade distances being most characteristic for the special case of 50% PCDPL's content compared to the other samples (Figures 10a and 10b) displaying an approximately higher pore size distribution. The visual inspiration of the impact fracture surface of the composite samples shown in Figures 10c and 10d regardless of the composite content, presented particle-sized agglomerates, indicative of dispersion, which likely resulted in improved strength. In addition, the morphological structure shown in Figure 10d, contributes to increased levels of mechanical adhesion and even molecular diffusion within the composite can be translated into improved mechanical behavior.

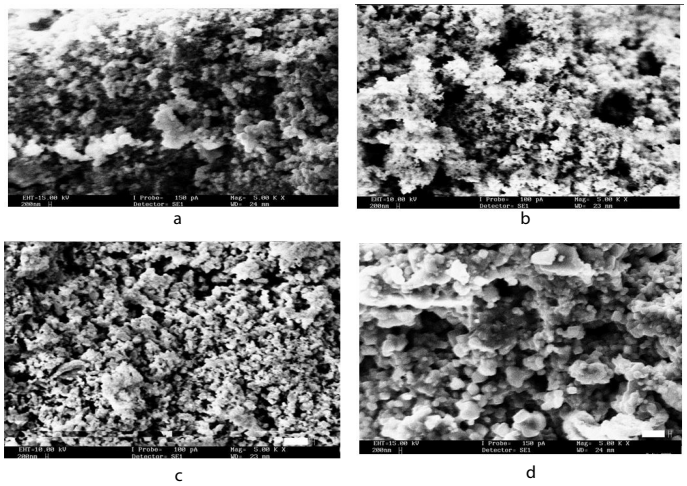


**Figure 10.** SEM micrographs of CCOC pellets prepared at 1000 ℃. **a)** 90% PCDPLs, **b)** 80% PCDPLs, **c)** 70% PCDPLs and d) 50% PCDPLs.

## Bulk density and young's modulus

Table 4 presents the results for CCOC pellets made both before and after pyrolysis methods. It indicates that while the bulk solid density arose after carbonization, the apparent density only marginally dropped despite the composites losing a large amount of weight and experiencing significant volume shrinkage. Also, density increased rapidly with decreasing PCDPLs% content, suggesting that the maximum density had been achieved: graphitic microstructures or disordered graphitic microstructures. Similar observations have been found for the bulk density of the Composite yield (Yield) varied from 38.1% to 64.2% with the increase (MKS+CU) % concentration. The composite yield for the untreated sample (PCDPLs 100%) is that of activated carbon from olive stone activated by phosphoric acid [39,40]. On the other hand, the YM of carbon pellets slightly increased from 6.35 GPa to 21.53 GPa with an increase of (MKS+CU) % content. It is much smaller than that of glassy carbon S-K (35 GPa) and pure graphite (27 GPa) indicating that the composite produced is still porous. Additionally, the YM of CCOC is treated with 90% and 100% in agreement with untreated solid carbon pellets activated carbon pellets from date palm leaves activated with potassium hydroxide [31] as shown in Table 3.

Note: a is for solid carbon pellet from date palm leaves prepared by different compression pressure [11], b is for activated carbon from olive stones [12]. Visual inspiration of the composites processed with 50% PCDPLs content present the same data of pure graphitic structure such as bulk density and YM. In addition, the ideal combination of these three materials, i.e. biomass PCDPLs+MKS and Cu filler, with distinct contents gives rise to YM with superior improvement in crystalline structure. This behavior is most likely because of the addition of MKS and Cu as a hard filler to the PCDPLs which results in increased mechanical properties of the product as a whole, thus increasing occupational mobility as a result of improved mechanical performance.

## Electrical Conductivity (EC)

Figures 11 and 12 represent the variation of Electrical Conductivity (EC) depending on frequency (EC) (real part (EC (r) and imaginary part (EC(i)) for the selected carbon composite samples having concentrations of (50%, 60%, 70% and 80%) PCDPLs at room temperature (298 K). An important observation is that the real part shows a marked increase at low frequency, and then it decreases at high frequency, while the imaginary part decreased markedly with increasing the frequency dependence and the intercept at zero frequency represents the DC resistance [6].

The Cole-Cole graphical plot of the imaginary part (EC(i)) plotted against the real part at different frequencies, the results explained the semicircular sketch shape and the size, with a narrow threshold range from 0 to 1.3, as shown in Figure 13 and Table 5, which is explained the theoretical behavior of Debye method [6-8]. Such behavior shows that the electrical conductivity increased with the reduction of PCDPls% concentration, but the conductivity is still low, revealing that carriers, as a resultant of a random distribution or disordered structures.

**Table 4.** PCDPLs weight, ($W_1$, $W_2$), density ($P_1$, $P_2$), composite yield (C.Yield) and YM of CCOC pellets before and after carbonization process.

| | Grain pellet | | After carbonization | | | |
|---|---|---|---|---|---|---|
| BCDPLs S % | $W_1$ (g) | $P_1$ (g/cm³) | $W_2$ (g) | $P_2$ (g/cm³) | C.Yield % | YM (GPa) |
| 50 | 1.00±0.01 | 1.941±2.01 | 0.642± 1.47 | 1.800±2.83 | 64.2 | 21.50 |
| 60 | 1.00±0.01 | 1.896± 1.06 | 0.593±2.01 | 1.615±1.53 | 61.3 | 19.29 |
| 70 | 1.01±0.01 | 1.67± 2.05 | 0.562±1.26 | 1.488±2.61 | 56.2 | 17.78 |
| 80 | 1.01±0.01 | 1.469± 3.03 | 0. 506±2.03 | 1.311±2.45 | 50.6 | 15.66 |
| 90 | 1.01±0.03 | 1.417± 2.04 | 0.466±1.68 | 1.228±1.76 | 46.6 | 11.09 |
| 100 | 1.01±0.10 | 1.231± 2.12 | 0.381 | 0.928±3.22 | 38.1 | 6.731 |
| Abbas FM, et al. [10] | | | | 1.083- 1.323 | | 5.21- 6.39 |
| Abbas FM, et al. [31] | | | | 0.940 -1.348 | | 7.79- 10.18 |
| Kosicek M, et al. [38] | | | | | 31-36 | |
| Graphite | | | | 2.226 | | 27.00 |
| Glassy carbon (Sigradur K), Abbas FM, et al. [10] | | | | 1.54 | | 35.70 |

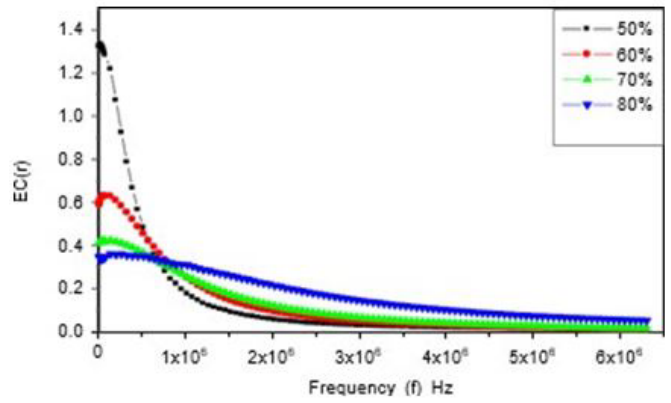


**Figure 11.** EC(r) real part *vs*. frequency (Hz).

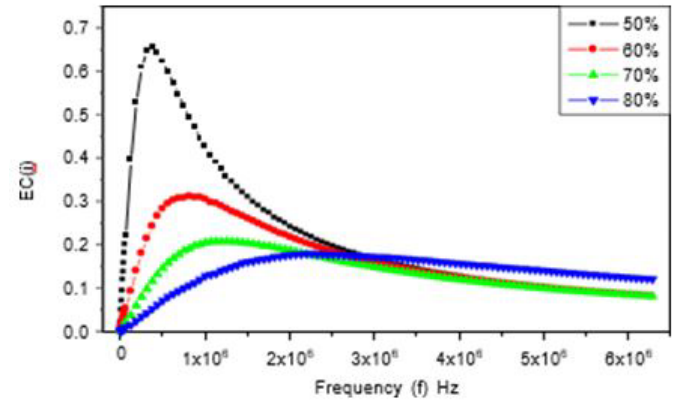


**Figure 12.** EC(i) imaginary part *vs*. frequency (Hz).

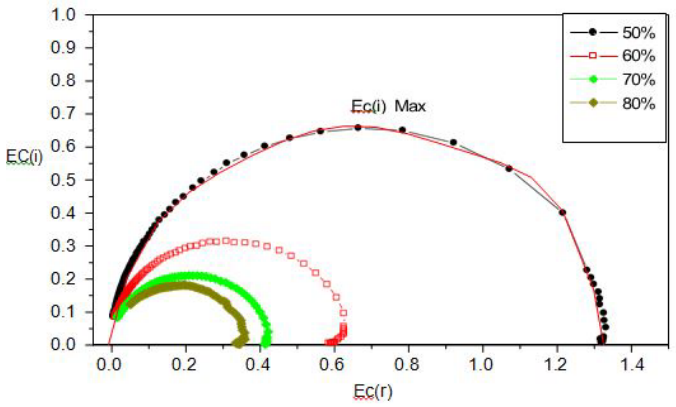


**Figure 13.** EC(r) *vs*. EC(i).

**Table 5.** Ec (i) max and Ec (r) max as a function of PCDPL% concentrations.

| PCDPL% | Ec(i) Max | EC(r) Max |
|---|---|---|
| 50 | 0.650 | 1.323 |
| 60 | 0.306 | 0.619 |
| 70 | 0.212 | 0.425 |
| 80 | 0.174 | 0.356 |

## Conclusion

According to the XRD analysis, every Carbon Composite Pellets (CCPs) that was produced has a polycrystalline structure. Therefore, MKS and Cu treatment on the PCDPLs powders were found to be effective in enhancing the crystallite structure, SL, YM of the composite produced, while showing a reduction in the specific surface area due to increasing the (MKS+Cu) contents. The results also show that it's possible to use a cubic volume granular structure to characterize the spring length between two cubic granular structures to avoid cracks. The frequency dependent conductivity was successful in the Cole-Cole plot, and we found that it followed the Debye theoretical behavior. The resulting composite materials are differentiated by properties to encounter various applications. The ideal combination of these three materials, i.e. biomass PCDPLs+MKS and Cu filler, with distinct contents gives rise to nanoparticle-composite carbon with superior improvement in crystalline structure and mechanical performance.

## Acknowledgement

The authors extend their appreciation to the Deanship of Research and Graduate Studies at King Khalid University for funding this work through small- group research under grant number RGP 1/50/45.

## Conflict of Interest

None.

## References

1. Barile, C. C. F. D. C. C., C. Casavola and F. De Cillis. "Mechanical comparison of new composite materials for aerospace applications." *Compos B Eng* 162 (2019): 122-128.
2. Rawat, Shivam, Rakesh K. Mishra and Thallada Bhaskar. "Biomass derived functional carbon materials for supercapacitor applications." *Chemosphere* 286 (2022): 131961.
3. Borenstein, Arie, Ortal Hanna, Ran Attias and Shalom Luski, et al. "Carbon-based composite materials for supercapacitor electrodes: A review." *J Mater Chem A* 5 (2017): 12653-12672.
4. Iernutan, Razvan Andrei, Florin Babota and Raluca Istoan. "Carbon fibre reinforced aluminium mesh composite materials." *Procedia Manuf* 32 (2019): 901-907.
5. Ishak, M. M., M. Deraman, I. A. Talib and N. H. Basri, et al. "Effect of carbonization temperature on the physical and electrochemical properties of supercapacitor electrode from fibers of oil palm empty fruit bunches." *AIP Conf Proc* (2015).
6. Yu, HaNa, Marco L. Longana, Meisam Jalalvand and Michael R. Wisnom et al. "Pseudo-ductility in intermingled carbon/glass hybrid composites with highly aligned discontinuous fibres." *Compos - A: Appl Sci Manuf* 73 (2015): 35-44.
7. Zhao, Qian, Kai Zhang, Shuang Zhu and Hanyang Xu, et al. "Review on the electrical resistance/conductivity of carbon fiber reinforced polymer." *Appl Sci* 9 (2019): 2390.
8. Yichuan, W. A. N. G. "Raman Scattering of Grossular-Andradite Solid Solution." *J High Press Phys* 34 (2020).
9. Tadda, M. Abubakar, Amimul Ahsan, Abubakar Shitu and Moetaz ElSergany, et al. "A review on activated carbon: process, application and prospects." *J Adv Civ Eng Pract Res* 2 (2016): 7-13.
10. Abbas, Fatima Musbah, Zehbah Ali Al Ahmad, Rehab Omer Elnour Elgezouly and Abubaker Elsheikh Abdelrahman. "Characterization of carbon pellets prepared from date palm leaves *(Phoenix dactylifera* L.*)* by compression pressure: X-ray diffraction measurements and applications." (2022).
11. Boyer, R. R., J. D. Cotton, M. Mohaghegh and dan RE Schafrik. "Materials considerations for aerospace applications." *MRS Bull* 40 (2015): 1055-1066.
12. Ou, Yu-jing, Chao Peng, Jun-wei Lang and Dan-dan Zhu, et al. "Hierarchical porous activated carbon produced from spinach leaves as an electrode material for an electric double layer capacitor." *New Carbon Mater* 29 (2014): 209-215.
13. Farma, Rakhmawati, Mohamad Deraman, A. Awitdrus and I. A. Talib, et al. "Preparation of highly porous binderless activated carbon electrodes from fibres of oil palm empty fruit bunches for application in supercapacitors." *Bioresour Technol* 132 (2013): 254-261.
14. Yue, Jing, Jiaqi Yu, Shaohua Jiang and Yiming Chen. "Biomass carbon materials with

porous array structures derived from soybean dregs for effective electromagnetic wave absorption." *Diam Relat Mater* 126 (2022): 109054.

15. Abbas, Fatima Musbah, Abubaker Elsheikh Abdelrahman and Abdul Kariem Arof. "Specific Surface area and spring lengths between two cubic volumes structure of the activated carbon pellets, from palm leaves, treated with KOH and carbonized at different temperature." (2023).
16. Şerban, Dan Andrei, Glenn Weber, Liviu Marşavina and Vadim V. Silberschmidt, et al. "Tensile properties of semi-crystalline thermoplastic polymers: Effects of temperature and strain rates." *Polym Test* 32 (2013): 413-425.
17. Hussain, Ahmad, Aamir Farooq, Mohammad Ismail Bassyouni and Hani Hussain Sait, et al. "Pyrolysis of Saudi Arabian date palm waste: A viable option for converting waste into wealth." (2014).
18. Migneault, Sébastien, Ahmed Koubaa, Patrick Perré and Bernard Riedl. "Effects of wood fiber surface chemistry on strength of wood–plastic composites." *Appl Surf Sci* 343 (2015): 11-18.
19. Lazrak, Charaf, Bousselham Kabouchi, Maryama Hammi and Abderrahim Famiri, et al. "Structural study of maritime pine wood and recycled High-Density Polyethylene (HDPEr) plastic composite using Infrared-ATR spectroscopy, X-ray diffraction, SEM and contact angle measurements." *Case Stud Constr Mater* 10 (2019): e00227.
20. Abdelrahman, Abubaker Elsheikh, Fatima Musbah Abbas and Abdul Kariem Arof. "Crystallite Parameters, Amorphous Contents and Surface Functional Groups, Contents of Activated Carbon Prepared from KOH Treated Pre-Carbonized Date Palm Leaves (*Phoenix dactylifera L.*)." (2023).
21. Tey, J. P., A. K. Arof, M. A. Yarmo and M. A. Careem. "Activated carbon from bio-wastes of durian fruits as Active material for electrodes of electric double-layer capacitors." *J New Mater Electrochem Syst* 18 (2015).
22. Allaker, Robert P. and Zhiyu Yuan. "Nanoparticles and the control of oral biofilms." Nanobiomaterials in Clinical Dentistry (2019): 243-275.
23. Starowicz, Z., K. Gawlińska–Nęcek, R. P. Socha and Tomasz Płociński, et al. "Materials studies of copper oxides obtained by low temperature oxidation of copper sheets." *Mater Sci Semicond Process* 121 (2021): 105368.
24. Verma, Nishant and Nikhil Kumar. "Synthesis and biomedical applications of copper oxide nanoparticles: An expanding horizon." *ACS Biomater Sci Eng* 5 (2019): 1170-1188.
25. Masroor, Sheerin. "Basics of metal oxides: Properties and applications." Inorganic Anticorrosive Materials (2022): 85-94.
26. Zhan, Jiye, Minghua Chen and Xinhui Xia. "Controllable synthesis of copper oxide/carbon core/shell nanowire arrays and their application for electrochemical energy storage." *Nanomater* 5 (2015): 1610-1619.
27. Cao, F., X. H. Xia, G. X. Pan and J. Chen, et al. "Construction of carbon nanoflakes shell on CuO nanowires core as enhanced core/shell arrays anode of lithium ion batteries." *Electrochim Acta* 178 (2015): 574-579.
28. Yang, Zhibo, Desheng Wang, Fei Li and Dequan Liu, et al. "Facile synthesis of CuO nanorod for lithium storage application." *Mater Lett* 90 (2013): 4-7.
29. Fan, Zhaoyang, Jin Liang, Wei Yu and Shujiang Ding, et al. "Ultrathin NiO nanosheets anchored on a highly ordered nanostructured carbon as an enhanced anode material for lithium ion batteries." *Nano Energy* 16 (2015): 152-162.
30. Emmerich, F. G. "Application of a cross-linking model to the Young's modulus of graphitizable and non-graphitizable carbons." Carbon 33 (1995): 47-50.
31. Abbas, Fatima Musbah, Abubaker Elsheikh Abdelrahman and Abdul Kariem Arof. "Characterization of the crystallites parameters, specific sur-face area, young's modulus and spring length of the cubic granular Volume microstructures of the activated carbon pellets from date palm leaves treated with KOH." (2023).
32. Betancourt-Galindo, R., P. Y. Reyes-Rodriguez, B. A. Puente-Urbina and C. A. Avila-Orta, et al. "Synthesis of copper nanoparticles by thermal decomposition and their antimicrobial properties." *J Nanomater* 2014 (2014): 980545.
33. Devi, Henam Sylvia and Thiyam David Singh. "Synthesis of copper oxide nanoparticles by a novel method and its application in the degradation of methyl orange." *Adv Electr Electron Eng* 4 (2014): 83-88.
34. Dhyani, Vaibhav and Thallada Bhaskar. "A comprehensive review on the pyrolysis of lignocellulosic biomass." *Renew Energy* 129 (2018): 695-716.
35. Robinson, Kyle P. "AC impedance spectroscopy on copper phthalocyanine thin films." (2013).
36. Abubakar, Abdullahi Musa, Fatih Biryan and Kadir Demirelli. "Electrical properties, characterization and preparation of composite materials containing a polymethacrylate with α-naphthyl side group and nanographene fillers." *J Thermoplast Compos Mater* 34 (2021): 102-125.
37. Abdelrahman, Abubaker Elsheikh, Fatima Musbah Abbas and Selma Elsheikh Abdelrahman. "Crystallites dimensions and electrical conductivity of Solid Carbon Pellets (SCPs) from date palm leaves (*Phoenix dactylifera* L.)." *Ajrsp* 4 (2023): 05-21.
38. Kosicek, Martin, Janez Zavasnik, Oleg Baranov and Barbara Setina Batic, et al. "Understanding the growth of copper oxide nanowires and layers by thermal oxidation over a broad temperature range at atmospheric pressure." *Cryst Growth Des* 22 (2022): 6656-6666.
39. Nor, N. S. M., Mohamad Deraman, N. H. Basri and B. N. M. Dollah, et al. "Supercapacitor activated carbon electrode from composite of green monoliths of KOH-treated pre-carbonized oil palm empty fruit bunches and $HNO_3$-treated graphite." *Adv Mater Res* 1112 (2015): 303-307.
40. Dolah, B. N. M., M. A. R. Othman, M. Deraman and N. H. Basri, et al. "Supercapacitor electrodes from activated carbon monoliths and carbon nanotubes." *J Phys Conf Ser* (2013).

**How to cite this article:** Abbas, Fatima Musbah, Ahlam Khalofa, Hanan Musbah Abbas and Abubaker Elsheikh Abdelrahman. "Carbon/Copper Oxide Composite (CCOC) from Date Palm Leaves, (Phoenix Dactyliferous L.), Tropical Fruit, Mata Kucing Seeds (Euphoria Malaiensis) and Cu Powder." *Mol Biol* 14 (2025): 470.

## Appendix A

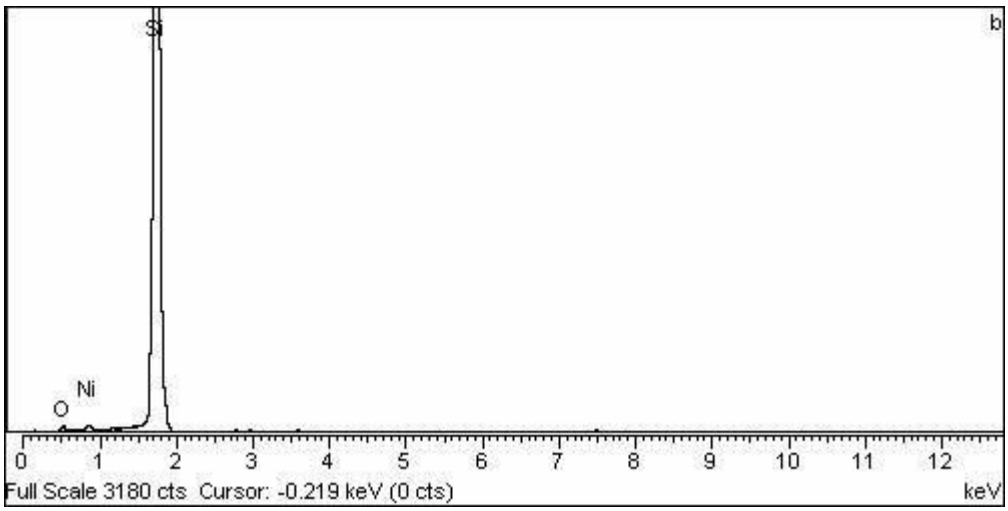


**Appendix A.** EDXRD data for Ni/$SiO_2$ layer.

## Appendix B

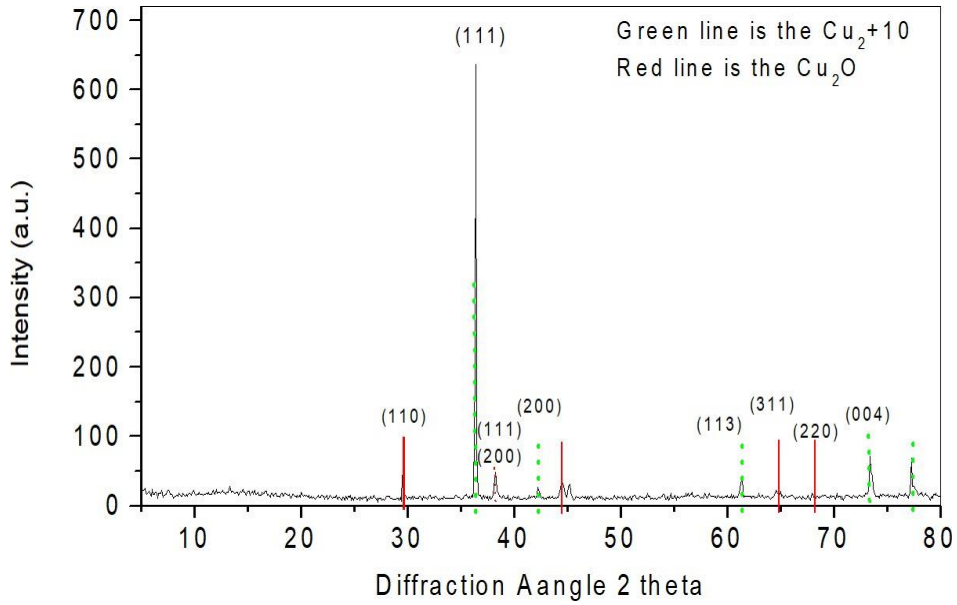


**Appendix B.** XRD data for Cu plate surface.